Journal of Applied Polymer Science

Modeling of the Atom Transfer Radical Polymerization for Preparing Novel Fluorosilicone Diblock Copolymers in a Semi-Batch Reactor

Yao Huang,[1] Yin-Ning Zhou,[2] Qing Zhang,[2] Zheng-Hong Luo[1,2]

[1]Department of Chemical and Biochemical Engineering, College of Chemistry and Chemical Engineering, Xiamen University, Xiamen 361005, China

[2]Department of Chemical Engineering, School of Chemistry and Chemical Engineering, Shanghai Jiaotong University, Shanghai, 200240, China

Correspondence to: Q. Zhang (E-mail: alqzhang@sjtu.edu.cn)

ABSTRACT: To investigate the process for the preparation of well-defined poly-dimethylsiloxane-*b*−2,2,3,3,4,4,4-heptafluorobutylmetharylate block copolymers via a macroinitiator initiated atom transfer radical polymerization (ATRP), a model for the batch and semi-batch ATRP process was presented based on the method of moments. The ATRP mechanism, the diffusion limitation, and the reactor choice were considered in the model. Besides, the polymer molecular weight, monomer conversion, and polymer polydispersity index as a function of polymerization time were described by this model. The model was validated by comparing simulated results with experimental data and was also used to investigate the effects of diffusion limitation and reactor choice (i.e., batch and semi-batch reactors). © 2013 Wiley Periodicals, Inc. J. Appl. Polym. Sci. 130: 3473–3481, 2013

KEYWORDS: theory and modeling; kinetics; radical polymerization

Received 8 November 2012; accepted 1 June 2013; Published online 23 June 2013
DOI: 10.1002/app.39602

INTRODUCTION

Fluorosilicone block polymers which combine the unique properties of silicone polymers and those of fluorinated polymers, such as polydimethylsiloxane-*b*-2, 2,3,3,4,4,4-heptafluorobutylmetharylate (PDMS-*b*-PHFBMA)[1–3] have been achieved mainly by living polymerization techniques[4] including living radical polymerization (LRP).[5–9] Much interest has been devoted to LRP recently, as it provides greater monomer diversity and less stringent reaction conditions.[10] Among the LRP techniques, atom transfer radical polymerization (ATRP) can be applied to prepare well-defined block copolymers with easy controllable polymer architecture, molecular weight and molecular weight distribution, and it only needs moderate experimental condition.[11] Recently, a series of PDMS-*b*-PHFBMA diblock copolymers were prepared by the ATRP.[7–9] The excellent properties, including low surface energy, self-assembly, and microphase separation behavior have been investigated deeply and precisely. But the polymerization was operated in a batch reactor and the polymerization kinetics was not involved.[7–9] The effects of the diffusion limitation as well as the reactor choice (i.e., batch and semi-batch reactors) were not mentioned, although they are very important for the polymerization kinetic study/modeling and may influence the polymerization results greatly.[12,13] Furthermore, the semi-batch reactor is much flexible for the preparation of polymers,[14] for example, Zhou and Luo recently used the semi-batch Cu(0)-mediated LRP technique to produce linear gradient copolymers.[15] Another study published by the same authors clearly demonstrated the effect of synthesis methodology on the molecular structure. Based on theory models, batch copolymerization leads exclusively to random copolymer, and di-block copolymer can be produced by sequential homopolymerization. Meanwhile, semi-batch polymerization based on the developed model can easily be performed to create polymeric materials having a gradient composition.[16] Herein, we pay special interest to the kinetic modeling of the production of fluorosilicone diblock copolymers, which is important in polymerization reaction engineering and also can be promoted to other polymerization systems.

Models for ATRP have been developed by several research groups.[17–21] The previous work was done in a batch reactor. It is notable that the models developed initially for ATRP did not contain diffusion limitation,[17] and the effect of diffusion limitation on controlling of ATRP was studied later on.[18,19] Zhang and Ray developed a comprehensive mathematical model for ATRP of styrene to provide a tool for the study of process development and design issues.[20] In their work, polymerization results in batch, semi-batch, and a series of continuous tank reactors were analyzed. Wang et al. developed a model and

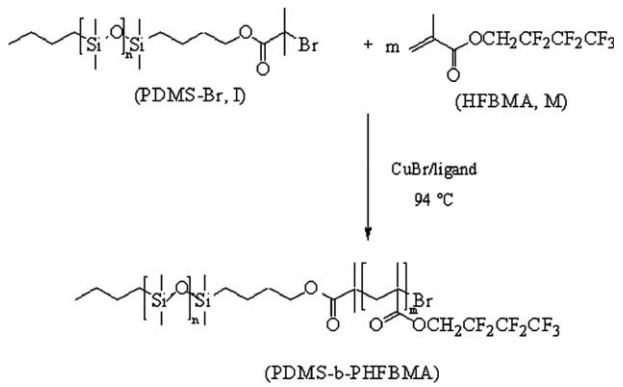

Scheme 1. Synthetic scheme of the PDMS-*b*-PHFBMA diblock copolymers via ATRP.

simulated copolymerization system with various reactivity rations in a semi-batch reactor to control of gradient copolymer composition in ATRP.[21] Recently, Zhou and Luo reported a systematic study, which was carried out on the preparation of poly(methyl methacrylate-*grad*-2-hydroxyethyl methacrylate) with simultaneously tailor-made chain composition distribution and T_g through semi-batch atom transfer radical polymerization.[22]

In this work, we develop a comprehensive mathematical model for the solution ATRP of HFBMA using the PDMS-Br macroinitiator. Moreover, our present work is focused on the investigation of the effects of the diffusion limitation as well as the reactor choice on the polymerization process.

EXPERIMENTAL

The experimental section in this work is similar to those reported in our previous work[7,22] and Sun et al.'s work.[23,24] Herein, in order to keep the completeness of the study, the experimental section was still described here in brief.

Materials

Monocarbinol-terminated polydimethylsiloxane (PDMS-OH, with an average molecular weight of 5000 g/mol) and 2-bomo-2- methylpropionylbromide (98%) were obtained from A Better Choice for Research Chemicals (ABCR) GmbH & Co. KG. Triethylamine was supplied by Sinopharm Chemical Reagent Co, Ltd. (SCRC 99%) and stored over 4-Å molecular sieves. *N*-Propylamine (98%) and pyridine-2-carboxaldehyde (99%) were obtained from ABCR. HFBMA (98%) purchased from Lancaster was washed with 5% aqueous NaOH solution to remove the inhibitor. Copper (I) bromide (98%) obtained from Aldrich was purified to remove Cu (II) by precipitation from the concentrated HBr acid by addition of water under nitrogen atmosphere. All other reagents and solvents were obtained from SCRC and used without further purification.

Synthesis of PDMS-*b*-PHFBMA Diblock Copolymers via Batch ATRP

Polydimethylsiloxane macroinitiator (PDMS-Br, R_0X, I) and *N*-(*n*-propyl)-2-pyridinylmethanimine (ligand) were synthesized as reported previously.[7] The PDMS-*b*-PHFBMA diblock copolymers were prepared by batch ATRP using PDMS-Br macroinitiator (Scheme 1). It should be emphasized that the number-average molecular weight and molecular weight distribution of PDMS-Br measured by gel permeation chromatography (GPC) are 5650 g/mol and 1.03, whilst the molecular weight calculated by ^{1}H-NMR is 5150 g/mol.[7] The typical synthesis process is as follows: First, the macroinitiator PDMS-Br (I), toluene, ligand, and CuBr were added into a dried round-bottom flask equipped with a magnetic stirrer bar. Next, the flask was purged with N_2 and then vacuumized. After three repetitions, a predetermined amount of HFBMA was added with an injector under N_2. The flask was placed in a preheated and thermally regulated oil bath at 94°C. All the polymerization conditions are summarized in Table I.

Synthesis of PDMS-*b*-PHFBMA Diblock Copolymers via Semi-Batch ATRP

Different from the method above, the present synthesis is via semi-batch ATRP which is similar to previous works.[22–24] The deoxygenized monomer (HFBMA, M) was continuously fed to the flask by metering pump. The feeding rate ($V_f = 1.2$ μL/min) is determined according to the simulation result, which corresponds to targeted monomer conversion within the batch reaction time. Other polymerization conditions are the same to the batch process.

Samples were taken out from the flask at regular intervals with a syringe and then handled as described as follow: Diluted with THF, and precipitated in methanol, the obtained polymer was rinsed with methanol for several times and dried to constant weight under vacuum at 50°C. The monomer conversion was measured by gravimetry.

Measurements

The polymers samples were measured by nuclear magnetic resonance (^{1}H-NMR) on a Bruker AV400 NMR spectrometer in deuterated chloroform. The molecular weight (M_n) and molecular weight distribution (M_w/M_n, polydispersity index (PDI)) of the polymer samples were determined at 40°C by GPC. GPC was carried out using tetrahydrofuran (THF) at a flow rate of 1 mL/min, with a Waters 1515 isocratic HPLC pump equipped with a Waters 2414 refractive index detector and three Waters Styragel HR columns (1 × 104, 1 × 103, and 500 Å pore sizes). Monodisperse polystyrene standard samples were used for calibration.

MODEL DEVELOPMENT

Scheme and Kinetic Equations for Batch ATRP of HFBMA

As described in Scheme 1, the present ATRP process to prepare PDMS-*b*-PHFBMA diblock copolymers consists of one-step ATRP using the PDMS-Br macroinitiator. In order to simplify the modeling work in the specific ATRP system. The following three assumptions, which have been proved to be sufficient for

Table I. Recipes Used for the Experimental Runs of ATRP of HFBMA

Expt.	HFBMA (mL)	Toluene (mL)	PDMS-Br (g)	Cu(I)Br (g)	Ligand (mL)
1	1.06	6.0	1.08	0.03	0.06
2	2.54	8.0	1.08	0.03	0.06

describing the ATRP process, are applied[18]: (1) the value of the rate constant for each step is independent on chain length; (2) only chain transfer to monomer is considered; (3) the value of the initiator-activation rate constant is equal to that of the dormant. Therefore, elementary reactions can be obtained as follows:

$$\text{Chain initiation:} \quad R_0X + C \overset{k_a/k_{da}}{\leftrightarrow} R_0\cdot + CX \tag{1}$$

$$R_0\cdot + M \xrightarrow{k_{in}} R_1\cdot \tag{2}$$

$$\text{ATRP equilibrium:} \quad D_i + C \overset{k_a/k_{da}}{\rightarrow} R_i\cdot + CX, \tag{3}$$

$$\text{Chain propagation:} \quad R_i\cdot + M \xrightarrow{k_p} R_{i+1}\cdot, \tag{4}$$

$$\text{Chain transfer to monomer:} \quad R_i\cdot + M \xrightarrow{k_{tr}} P_i + R\cdot, \tag{5}$$

$$\text{Chain termination:} \quad R_i\cdot + R_j\cdot \xrightarrow{k_{tc}} P_{i+j}, \tag{6}$$

$$R_i\cdot + R_j\cdot \xrightarrow{k_{td}} P_i + P_j, \tag{7}$$

There are three types of chain species involved in the ATRP: (1) dormant radical chain, D_i, (2) propagating radical chain, $R_i\cdot$, and (3) dead chain, P_i. For these species, the following molar balance equations/kinetic equations can be derived:

$$\text{for } D_i: \quad \frac{d[D_i]}{dt} = -k_a[D_i][C] + k_{da}[R_i\cdot][CX], \tag{8}$$

for $R_i\cdot$:

$$i=1, \quad \frac{d[R_1\cdot]}{dt} = k_a[D_1][C] - k_{da}[R_1\cdot][CX] - k_p[R_1\cdot][M] - k_{tr}[R_1\cdot][M] - (k_{tc}+k_{td})[R_1\cdot]\sum_{i=1}^{\infty}[R_i\cdot], \tag{9}$$

$$i \geq 2, \quad \frac{d[R_i\cdot]}{dt} = k_a[D_i][C] - k_{da}[R_i\cdot][CX] + k_p[R_{i-1}\cdot][M] - k_p[R_i\cdot][M] - k_{tr}[R_i\cdot][M] - (k_{tc}+k_{td})[R_i\cdot]\sum_{i=1}^{\infty}[R_i\cdot], \tag{10}$$

for P_i:

$$i=1, \quad \frac{d[P_1]}{dt} = k_{tr}[R_1\cdot][M] + k_{td}[R_1\cdot]\sum_{i=1}^{\infty}[R_i\cdot], \tag{11}$$

$$i \geq 2, \quad \frac{d[P_i]}{dt} = k_{tr}[R_i\cdot][M] + k_{td}[R_i\cdot]\sum_{i=1}^{\infty}[R_i\cdot] + \frac{k_{tc}}{2}\sum_{r=1}^{i-1}[R_r\cdot][R_{i-r}\cdot]. \tag{12}$$

Table II. Differential Moment Equations

Zeroth order moments	Dormant chains	$\frac{d\lambda_0}{dt} = -k_a[C][\lambda_0] + k_{da}[CX][\mu_0]$
	Propagating radical chains	$\frac{d\mu_0}{dt} = k_a[C][\lambda_0] - k_{da}[CX][\mu_0] - k_{tr}[M][\mu_0] - (k_{tc}+k_{td})[\mu_0][\mu_0]$
	Dead chains	$\frac{d\tau_0}{dt} = k_{tr}[M][\mu_0] + k_{td}[\mu_0][\mu_0] + \frac{k_{tc}}{2}[\mu_0][\mu_0]$
First-order moments	Dormant chains	$\frac{d\lambda_1}{dt} = -k_a[C][\lambda_1] + k_{da}[CX][\mu_1]$
	Propagating radical chains	$\frac{d\mu_1}{dt} = k_a[C][\lambda_1] - k_{da}[CX][\mu_1] + k_p[M][\mu_0] - k_{tr}[M][\mu_1] - (k_{tc}+k_{td})[\mu_0][\mu_1]$
	Dead chains	$\frac{d\tau_1}{dt} = k_{tr}[M][\mu_1] + k_{td}[\mu_0][\mu_1] + k_{tc}[\mu_0][\mu_1]$
Second-order moments	Dormant chains	$\frac{d\lambda_2}{dt} = -k_a[C][\lambda_2] + k_{da}[CX][\mu_2]$
	Propagating radical chains	$\frac{d\mu_2}{dt} = k_a[C][\lambda_2] - k_{da}[CX][\mu_2] + k_p[M][\mu_0] + 2k_p[M][\mu_1] - k_{tr}[M][\mu_2] - (k_{tc}+k_{td})[\mu_0][\mu_2]$
	Dead chains	$\frac{d\tau_2}{dt} = k_{tr}[M][\mu_2] + k_{td}[\mu_0][\mu_2] + k_{tc}[\mu_0][\mu_2] + k_{tc}[\mu_1][\mu_1]$
Small molecules	HFBMA monomer	$\frac{dM}{dt} = -(k_p + k_{tr})[M][\mu_0]$
	Activator	$[C] = [C_0] - [CX]$
	Deactivator	$[CX] = [I_0] - [\lambda_0]$

Definition of Chain Moments and Derivation of Moment Equations

The methodology used in this study is an extension of Zhu et al.'s previous work on ATRP.[17] The moments of chain species are defined in eqs. (13–15):

$$\text{for D}_i: \quad \lambda_m = \sum_{i=1}^{\infty} i^m [\text{D}_i], \tag{13}$$

$$\text{for R}_i\cdot: \quad \mu_m = \sum_{i=1}^{\infty} i^m [\text{R}_i\cdot], \tag{14}$$

$$\text{for P}_i: \quad \tau_m = \sum_{i=1}^{\infty} i^m [\text{P}_i]. \tag{15}$$

The moment equations could be obtained by combining the moment definitions given in eqs. (13–15) with the population balance shown in eqs. (8–12). A complete set of moment equations can be derived as summarized in Table II. The polymerization kinetics or the chain properties such as monomer conversion (X), number-average molecular weight (M_n), weight-average molecular weight (M_w), and PDI can be readily described as follows:

$$\text{for } X: \quad X = \frac{[\text{M}]_0 - [\text{M}]_t}{[\text{M}]_0}, \tag{16}$$

$$\text{for } M_n: \quad M_n = \frac{\lambda_1 + \mu_1 + \tau_1}{\lambda_0 + \mu_0 + \tau_0} \times M_m + M_{n,\text{PDMS}}, \tag{17}$$

$$\text{for } M_w: \quad M_w = \frac{\lambda_2 + \mu_2 + \tau_2}{\lambda_1 + \mu_1 + \tau_1} \times M_m + M_{m,\text{PDMS}}, \tag{18}$$

$$\text{for PDI}: \quad \text{PDI} = \frac{M_w}{M_n}. \tag{19}$$

Combination of Reaction and Diffusion

In free-radical polymerization, when the polymerization proceeds to intermediate and high conversions, the reacting mixture becomes viscous and the reactants experience diffusion limitation.[23] However, it could be acceptable to provide that when the polymerization conversion is low, only the diffusion-controlled termination reactions are considered herein, and the effects of the diffusion limitation on other elementary reactions such as equilibrium, propagation, and transfer/deactivation are ignored.[18,19,25,26]

For the diffusion-controlled termination reactions, on the basis of an encounter-pair model, the relative contributions of chemical activation and diffusion to the termination rate constant can be described as follows[23,27,28]:

$$\frac{1}{k_{\text{tc}}} = \frac{1}{k_{\text{tc,chem}}} + \frac{1}{k_{\text{tc,diff}}} \tag{20}$$

$$\frac{1}{k_{\text{td}}} = \frac{1}{k_{\text{td,chem}}} + \frac{1}{k_{\text{td,diff}}} \tag{21}$$

Equations (20)–(21) describe the relative contributions of the chemically and diffusion-controlled termination reactions.

The $k_{\text{tc,chem}}$ and $k_{\text{td,chem}}$ of termination reaction step, which are involved in the free radical polymerization of BMA, are obtained from literature data (see Table IV).

The diffusion-controlled rate coefficients can be calculated using the following free-volume-based on Vrentas-Dual model and Smoluchowski equation[28]:

$$k_{\text{tc,diff}}\left(k_{\text{td,diff}}\right) = 4\,\pi\, R_d (D_{\text{md}} + D_{\text{rd}}) N_A, \tag{22}$$

where, R_d is the molecule interaction radius in solution, D_{md} and D_{rd} are the centroid and reaction diffusion coefficients, respectively. For R_d, it is the catch/reaction radius of active chain and can be determined by the electriferous capability of the active group included in the active chain. Accordingly, its value can be directly obtained by the corresponding covalent-bond length.[28] In this study, R_d is the summation of the covalent-bond length of the end-group of $R_i\cdot$ and the covalent-bond length of the end-group of $R_j\cdot$, namely, the twice value of the covalent-bond length of the end-group of $R_i\cdot$ or $R_j\cdot$. From eqs. (6), (7), it can be found that the terminations by combination or disproportionation are happened between two radicals. Therefore, $k_{\text{tc,diff}}$ and $k_{\text{td,diff}}$ can be considered to be equivalent. Namely,

$$k_{\text{tc,diff}} = k_{\text{td,diff}}. \tag{23}$$

In addition, D_{md} can be obtained via the following equation[27,28]:

$$D_{\text{md}} = D_0 \exp\left[-\frac{\left(\omega_m \bar{V}_m^* + \omega_s \bar{V}_s^* + \omega_p \bar{V}_p^*\right)}{\bar{V}_{\text{FH}}}\right] \exp\left(\frac{-E^*}{RT}\right), \tag{24}$$

where, $\bar{V}_m^*$, $\bar{V}_s^*$, $\bar{V}_p^*$ are described using the specific occupied volumes of monomer, solvent, and polymer, respectively and E^* is the critical energy which a molecule must possess to overcome the attraction force holding it to its neighbors. Here, when $E^* \approx 0$,[25,27] then the "zeta factor" $\exp\left(\frac{-E^*}{RT}\right)$ equals to 1.[29] Furthermore, the specific occupied volumes ($\bar{V}_{m,s,P}^*$) can be estimated as the specific volumes of monomer, solvent, and polymer at 0 K, which are as follows:

$$\bar{V}_m^* = V_m^0(0K), \tag{25}$$

$$\bar{V}_s^* = V_s^0(0K), \tag{26}$$

$$\bar{V}_P^* = V_P^0(0K), \tag{27}$$

where, $V_m^0(0K)$, $V_s^0(0K)$, and $V_P^0(0K)$ can be obtained via the group contribution method.[29] Furthermore, $\bar{V}_{\text{FH}}$ can be obtained based on eq. (28):

$$\bar{V}_{\text{FH}} = \omega_m \bar{V}_m + \omega_s \bar{V}_s + \omega_p \bar{V}_p, \tag{28}$$

where,

$$\bar{V}_i = \frac{K_{i,1}}{\gamma}\left(K_{i,2} + T - T_{g,i}\right), \qquad (i = m, s, \text{and } p) \tag{29}$$

And D_{rd} can be obtained via the following equation[27,28]:

$$D_{\text{rd}} = \frac{1}{2} k_p [\text{M}] \alpha^2. \tag{30}$$

Semi-Batch Reactor Model

Considering the choice of reactor, a reactor model for the semi-batch polymerization must be developed. Compared to the batch operation process, only the volume and concentration change of species need to be considered in the semi-batch operation process. In addition, a well-mixed isothermal tank reactor is assumed in this work. Furthermore, due to a trace amount of initiator and a constant volume of solvent, only feeding monomer and resulting polymer significantly contribute to the change

Table III. The Main Thermodynamic and Property Parameters and Their Values Applied in this Work

Parameters	Values	References
D_0	1.0×10^{-6}	29
R_d (m)	1×10^{-9}	30
α	1×10^{-10}	30
$\bar{V}_m^*$ (cm^3/g)	0.965	30
$\bar{V}_s^*$ (cm^3/g)	0.917	29
$\bar{V}_p^*$ (cm^3/g)	0.905	28
$\frac{K_{i,1}}{\gamma}$ (cm^3/g K), $i = m, s, p$		29
m	2.97×10^{-3}	
s	2.20×10^{-3}	
p	9.32×10^{-4}	
$K_{i,2} - T_{g,i}$(K), $i = m, s, p$		29
m	−160.38	
s	−102.72	
p	−81.0	
T(K)	368.15	30
N_A (mol^{-1})	6.022×10^{23}	Avogadro constant

of volume (V) and density (ρ) in the semi-batch operation process. Therefore, the mass balance equations for all entities can be worked out in the semi-batch reactor.

For the semi-batch reactor, the following mass balance equation can be derived:

$$\frac{dV}{dt} = V_f - \sum_{i=1}^{n} M_{m,i} R_{pi} \left(\frac{1}{\rho_{m,i}} - \frac{1}{\rho_p} \right) V. \tag{31}$$

where V_f is the volumetric flow rate of monomer into the reactor, $M_{m,i}$ is the molecular weight of i-type monomer and R_{pi} is the intrinsic propagating rate of i-type monomer.

In order to simplify the model, the change of volume that occurs during polymerization due to the difference of density between monomer ($\rho_{m,i}$) and polymer (ρ_p), is ignored. Accordingly, eq. (31) can be simplified as follows:

$$\frac{dV}{dt} = V_f, \tag{32}$$

Equation (33) can be obtained by integrating eq. (32):

$$V = V_0 + V_f t. \tag{33}$$

For the ith species in the semi-batch reactor, the following mass balance equation can be derived:

$$\frac{d(VC_i)}{dt} = V_f C_{if} + V R_i, \tag{34}$$

$$\text{i.e.,} \frac{dC_i}{dt} = \frac{1}{V} \left(V_f C_{if} - C_i \frac{dV}{dt} \right) + R_i. \tag{35}$$

Combining eqs. (32) and (35), the following equation can be obtained:

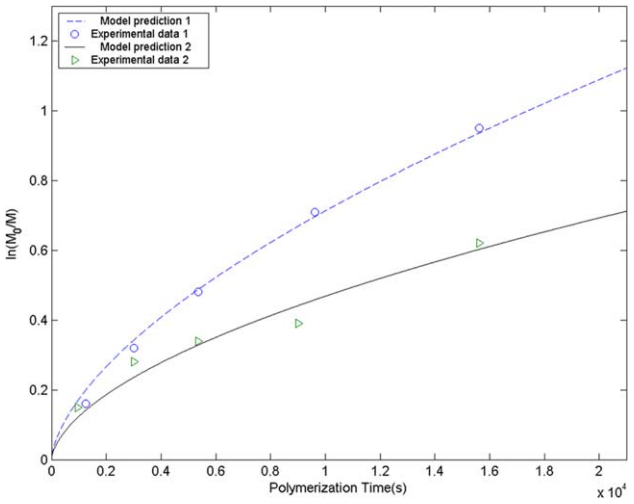

Figure 1. Comparison between models predictions and experimental data for batch solution ATRP of HFBMA: Monomer logarithmic conversion versus polymerization time (the molar ratio of each component of [M]/[I]/[Cu]/[ligand] = 25 : 1 : 1 : 2 or 60 : 1 : 1 : 2 stands for Experiment 1 or 2). [Color figure can be viewed in the online issue, which is available at wileyonlinelibrary.com.]

$$\frac{dC_i}{dt} = \frac{V_f (C_{if} - C_i)}{V} + R_i, \tag{36}$$

where, R_i is the intrinsic reaction rate of the ith species, as expressed in Table II. Therefore, eqs. (13–36) and equations. described in Table II constitute the semi-batch reactor model.

MODEL IMPLEMENTATION AND MODEL PARAMETERS ESTIMATION

Equations (8–36) and equations described in Table II comprised a set of stiff and ordinary differential equations. The ode23s-

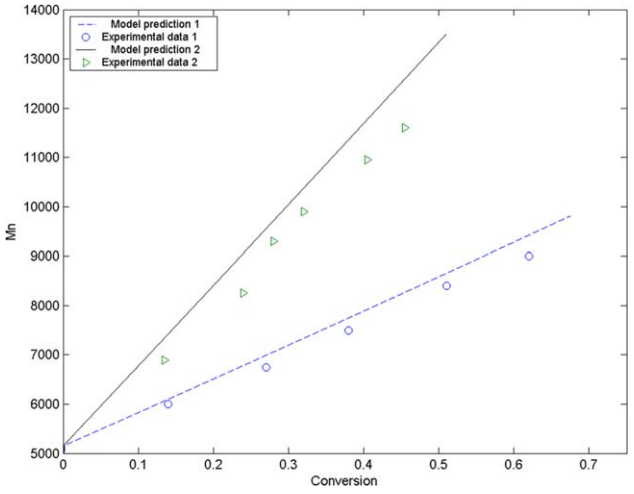

Figure 2. Comparison between models predictions and experimental data for batch solution ATRP of HFBMA: Number average molecular weight versus monomer conversion (the molar ratio of each component of [M]/[I]/[Cu]/[ligand] = 25 : 1 : 1 : 2 or 60 : 1 : 1 : 2 stands for Experiment 1 or 2). [Color figure can be viewed in the online issue, which is available at wileyonlinelibrary.com.]

Table IV. Kinetic Rate Constants of HFBMA ATRP Used in Simulation

Parameters	Values (L mol^{-1} s^{-1})	References
k_p	$3.80\times10^6\exp(-2754/T)$	31
k_{tr}	$1.56\times10^2\exp(-2621/T)$	31
k_t ($k_{tc} = 0.9\ k_t$; $k_{td} = 0.1\ k_t$)	$7.1\times10^9\exp(-2249/T)$	32,33
k_a	0.27	This work
k_{da}	2.05×10^7	This work

function provided in Matlab 6.5 software was used to solve the ordinary differential equations.

The main thermodynamic and characteristic parameters and their values applied in this work are listed in Table III. In addition, the kinetic constants were collected and listed in Table IV. Since the values of the bulk reaction kinetic constants are independent on the reactor choice, activating and deactivating kinetic data can be obtained from the batch polymerization experiments. These experimental data (batch process) described in Refs. 7,34 were used to estimate the activating and deactivating kinetic constants according to least-square method. Furthermore, it could be found that the fitting data and the experimental data are almost equal. Corresponding correlation coefficients (R^2) is close to 1 (>0.97). Here, two sets of representative results are shown in Figures 1 and 2. The obtained parameters are shown in Table IV.

RESULTS AND DISCUSSION

Comparison between Experimental Data and Simulated Data

By substituting the model parameters listed in Tables III and IV for related terms in the above model respectively, the simulated results are obtained.

Figures 3 and 4 illustrate the comparisons between the experimental and simulated data with two different initial recipes at the semi-batch polymerization condition (the two initial recipes are the same as those described at the above batch polymerization condition), which show a good agreement between the experimental data and the simulated results. The correlation coefficients for corresponding experimental data all exceed 0.97. Combining the above comparisons shown in Figures 1 and 2 corresponding to the batch polymerization condition, it can be found that the simulated data obtained via the kinetic modeling corresponding to the batch and the semi-batch polymerization conditions meet their corresponding experimental data well. Once the model was testified, it was used to investigate the effects of diffusion limitation and reactor choice (i.e., batch and semi-batch reactors) on the polymerization process.

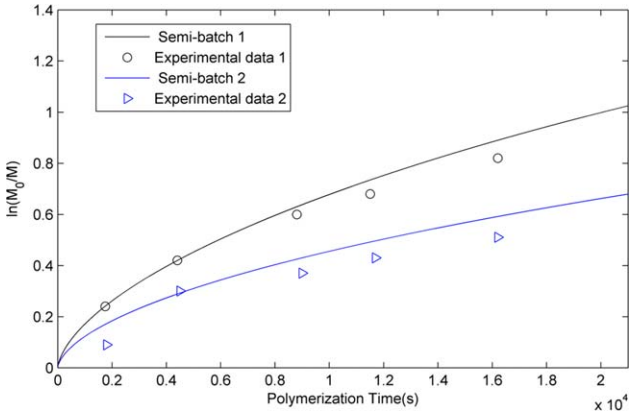

Figure 3. Model predictions and experimental data of monomer logarithmic conversion versus polymerization time for semi-batch feeding process (the molar ratio of each component of [M]/[I]/[Cu]/[ligand] = 25 : 1 : 1 : 2 or 60 : 1 : 1 : 2 stands for Experiment 1 or 2). [Color figure can be viewed in the online issue, which is available at wileyonlinelibrary.com.]

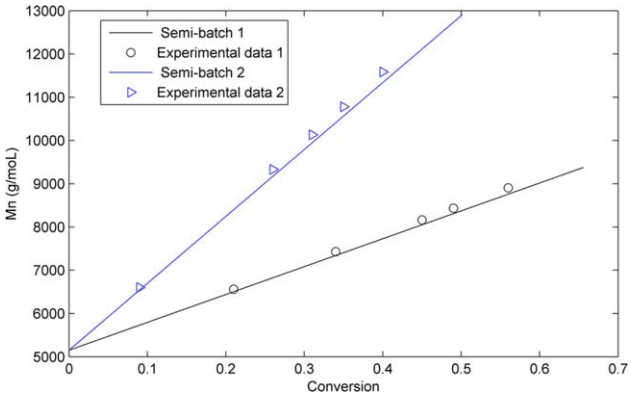

Figure 4. Model predictions and experimental data of number average molecular weight versus monomer conversion for semi-batch feeding process (the molar ratio of each component of [M]/[I]/[Cu]/[ligand] = 25 : 1 : 1 : 2 or 60 : 1 : 1 : 2 stands for Experiment 1 or 2). [Color figure can be viewed in the online issue, which is available at wileyonlinelibrary.com.]

Effect of Diffusion Limitation on Polymerization Kinetics at Semi-Batch Process

With two different initial recipes at the semi-batch polymerization condition, the model was used to simulate the ATRP process with or without concerning the diffusion limitation. Figures 5–7 show the effect of diffusion limitation on the polymerization kinetics at semi-batch condition. As a whole, Figures 5–7 prove that the effect of diffusion limitation on the

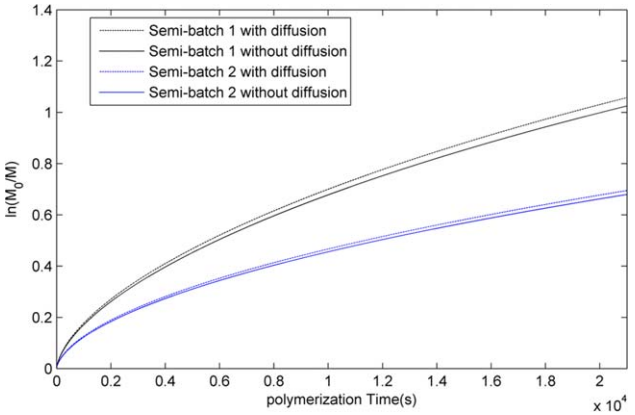

Figure 5. Monomer logarithmic conversion versus polymerization time for semi-batch feeding process with or without effects of diffusion limitation. [Color figure can be viewed in the online issue, which is available at wileyonlinelibrary.com.]

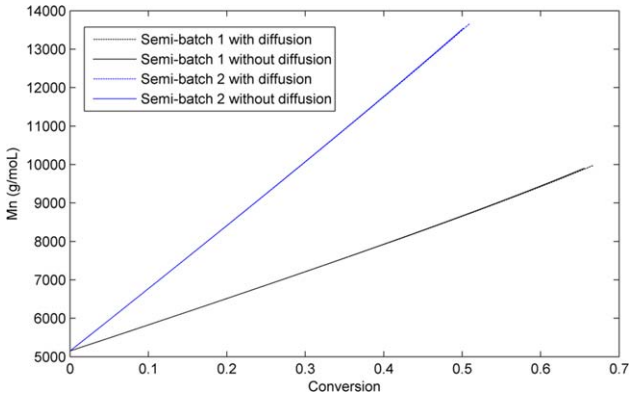

Figure 6. Number average molecular weight versus monomer conversion for semi-batch feeding process with or without effects of diffusion limitation. [Color figure can be viewed in the online issue, which is available at wileyonlinelibrary.com.]

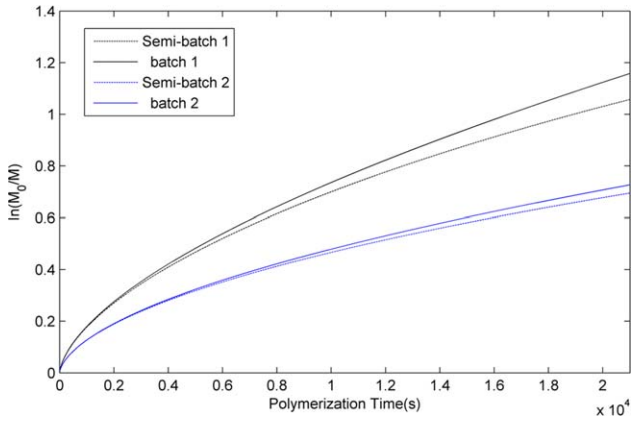

Figure 8. Comparison between semi-batch process and corresponding batch process: Monomer logarithmic conversion versus polymerization time, with the effects of diffusion limitation. [Color figure can be viewed in the online issue, which is available at wileyonlinelibrary.com.]

polymerization kinetics is not obvious due to the low conversion in our simulated system. In keeping with the conclusions from other references, this result demonstrates that the effect of diffusion can be ignored when the polymerization conversion does not reach very high values (>80%).[23,24] However, slight differences indicate that the effect of diffusion limitation still remain on the polymerization kinetics.

First, all curves in Figure 5 show that the polymerization conversion (i.e., the monomer logarithmic conversion in this study) increases with polymerization proceeding. When considering the diffusion limitation, one can find that the conversion increases and the increasing value is more and more obvious with the polymerization proceeding. It means that the diffusion can increase the polymerization rate. Furthermore, with the increase of polymerization conversion, the number average molecular weight (M_n) increases as shown in all curves in Figure 6. Meanwhile, at the same conversion, the distinction between the obtained M_ns, with or without considering the diffusion, is not obvious. Certainly, as described above, the difference can be ignored at low conversions. Next, the effect of diffusion on the polymer polydispersity (PDI) is also obtained via the above model and is shown in Figure 7. The PDI difference with and without concerning the diffusion limitation is almost unobservable. It is well known that ATRP proceeds in a controlled manner and is used to prepare polymers with narrow molecular weight distribution. Namely, the polymers obtained via ATRP have low PDIs (<1.2). Based on the low PDIs at low conversions, the effect of diffusion limitation on the resulting polymers can be ignored. Consequently, for the ATRP process for the production of PDMS-*b*-PHFBMA diblock copolymers in a semi-batch reactor, the effect of diffusion on the kinetics is not obvious and can be ignored at low conversions.

Effect of Reactor Choice on ATRP Kinetics

Herein, the effect of reactor choice (i.e., batch and semi-batch reactors) on polymerization kinetics is also simulated preliminary and the simulated results are shown in Figures 8–10.

Figure 8 shows the comparison of polymerization conversion versus polymerization time between semi-batch process and

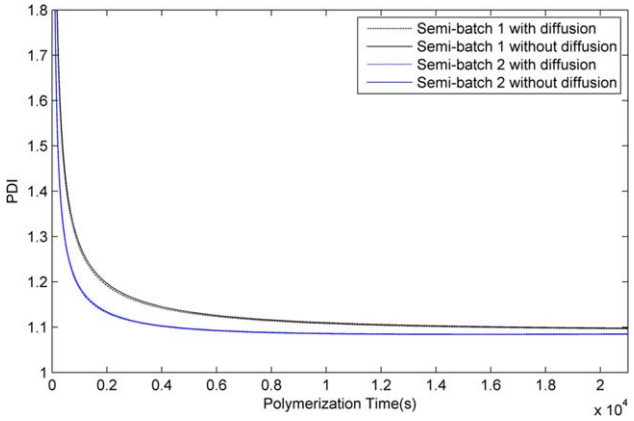

Figure 7. Polydispersity versus polymerization time for semi-batch feeding process, with or without effects of diffusion limitation. [Color figure can be viewed in the online issue, which is available at wileyonlinelibrary.com.]

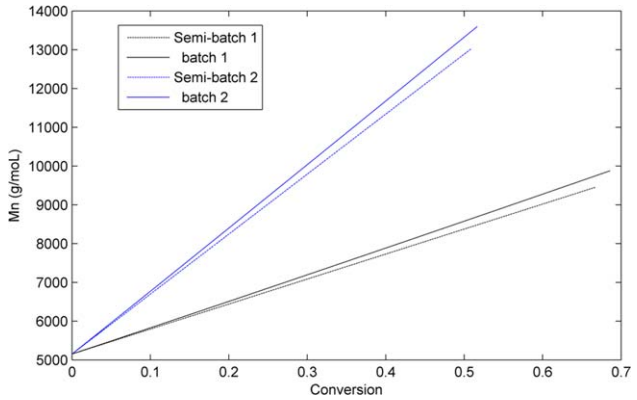

Figure 9. Comparison between semi-batch process and corresponding batch process: Number average molecular weight versus monomer conversion, with the effects of diffusion limitation. [Color figure can be viewed in the online issue, which is available at wileyonlinelibrary.com.]

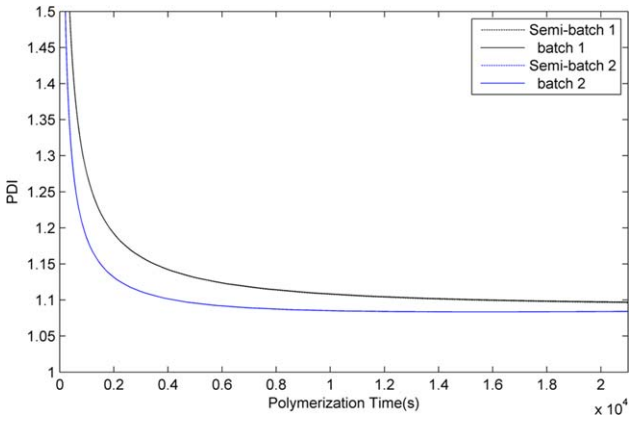

Figure 10. Comparison between semi-batch process and corresponding batch process: Polydispersity versus polymerization time, with the effects of diffusion limitation. [Color figure can be viewed in the online issue, which is available at wileyonlinelibrary.com.]

batch process at the same initial conditions. Although the effect of diffusion on the kinetics can be ignored at low conversions, the polymerization system will become diffusion controlled reaction at high conversion. Herein, we concern the diffusion limitation, namely, this simulated results (in batch and semi-batch reactors) are obtained with considering the diffusion limitation. In batch process, the polymerization conversion is higher than that in the corresponding semi-batch process with the same initial condition at the same reaction time. The slower reaction rate of semi-batch operation is stem from the relatively low concentration of reaction monomer in the reactor. From Figure 9, a linear relation between the average molecular weight and polymerization conversion can be found, which implies "living"/controlled characteristic of ATRP. In addition, it can be found that the polymer M_n in the semi-batch process is lower than that in the corresponding batch process at the same monomer conversion. The rate of transfer reaction (only chain transfer to monomer is considered) resulting from the low monomer concentration via semi-batch operation might be relatively lower than it via batch process, and thus the transfer reaction is suppressed. Another important feature of ATRP is the low PDI. In general, the polymer PDI is high at very low monomer conversion and rapidly decreases to values near 1.1 with the increase of polymerization conversion yet. Furthermore, our model prediction agrees well with this tendency, as described in Figure 10. The simulated results are almost the same in both batch and semi-batch process. Accordingly, the reactor choice has little influence on the PDI.

CONCLUSIONS

A model of the ATRP considering the diffusion limitation and the reactor choice for preparation of fluorosilicone diblock copolymers, poly-dimethylsiloxane-*b*-2,2,3,3,4,4,4-heptafluorobutylmetharylate block copolymers, has been developed. Next, activating and deactivating kinetic data are obtained from the batch polymerization experiments via least-square method. The model was preliminarily validated by comparing simulation results with experimental data obtained in semi-batch reactors, and was used to investigate the effects of diffusion limitation and reactor choice. The simulation results with or without diffusion limitation indicated that the diffusion effect described by the free volume theory has some influence on the reaction. The phenomenon of increasing the polymerization rate can be found in the polymerization process when considering the diffusion limitation. Certainly, the diffusion effect can be ignored from the viewpoint of engineering, especially at low conversions. In the aspect of reactor choice, the results showed that semi-batch operation keeps the monomer concentration at a relative low level, thus the transfer reaction is suppressed. Such advantage leads to higher molecular weight at the same conversion with respect to batch process. As a whole, the modeling of ATRP for preparing novel fluorosilicon diblock copolymers can help researchers to deeply understand the polymerization process.

NOMENCLATURE

α	average molecule radius, m
C	activator and catalyst at the lower oxidation state
C_i	concentration of the ith species, mol/L
CX	deactivator and catalyst at the higher oxidation state
D	dormant chain
D_{md}	centroid diffusion coefficients
D_{rd}	reaction diffusion coefficients
D_0	exponential factor
R_0X	macroinitiator
k_{α}	activation rate constant, L mol^{-1} s^{-1}
$k_{\mathrm{d}\,\alpha}$	deactivation rate constant, L mol^{-1} s^{-1}
k_p	chain propagation rate constant, L mol^{-1} s^{-1}
k_{tr}	chain transfer rate constant to monomer, L mol^{-1} s^{-1}
k_{tc}	chain termination rate constant by combination, L mol^{-1} s^{-1}
k_{td}	chain termination rate constant by disproportionation, L mol^{-1} s^{-1}
$K_{i,1}$	free-volume parameter, m^3/g K
M	monomer
λ_m	mth-order moment of dormant chain with
μ_m	mth-order moment of propagating radical
τ_m	mth-order moment of dead chain
M_m	monomer number-average molecular weight, g mol^{-1}
N_A	Avogadro constant, mol^{-1}
P	dead chain
$R_i\cdot$	propagating radical species
R_{d}	molecule interaction radius, m
R_{i}	intrinsic reaction rate of the ith species, mol L^{-1} s^{-1}
T	temperature, K
V	volume, m^3
V_f	volumetric feeding rate, m^3 s^{-1}
V^{*-}	specific occupied volume, m^3
V^{-}	specific free volume, m^3
ω	mass fraction
γ	overlap factor which accounts for shared free volume
ρ	density, kg m^{-3}

Subscripts

f	feed
i	chain length i or the ith species
j	chain length j

m monomer
p polymer
s solvent
0 initial state

ACKNOWLEDGMENTS

The authors thank the National Ministry of Science and Technology of China (No. 2012CB21500402), the National Natural Science Foundation of China (No. 21276213, 21076171). The authors also thank the anonymous referees for the helpful comments on this manuscript.

REFERENCES

1. Grunlan, M. A.; Mabry, J. M.; Weber W. P. *Polymer* **2003**, *44*, 981.
2. Ameduri, B.; Boutevin, B. Well-Architectured Fluoropolymers: Synthesis, Properties and Applications; Elsevier: Amsterdam, **2004**; p 103.
3. Luo, Z. H.; He, T. Y.; Yu, H. J.; Dai, L. Z. *Macromol. React. Eng.* **2008**, *2*, 398.
4. Bellas, V.; Iatrou, H.; Hadjichristidis, N. *Macromolecules* **2000**, *33*, 6993.
5. Guan, C. M.; Luo, Z. H.; Qiu, J. J.; Tang, P. P. *Eur. Polym. J.* **2010**, *46*, 1582.
6. Coessens, V. M. C.; Matyjaszewski, K. *J. Chem. Educ.* **2010**, *87*, 916.
7. Luo, Z. H.; He, T. Y. *React. Funct. Polym.* **2008**, *68*, 931.
8. Luo, Z. H.; Yu, H. J.; Zhang, W. *J. Appl. Polym. Sci.* **2009**, *113*, 4032.
9. Cheng, H.; Li, J. J.; Luo, Z. H. *J. Polym. Sci. Part A: Polym. Chem.* **2012**, *50*, 1249.
10. di Lena, F.; Matyjaszewski, K. *Prog. Polym. Sci.*, **2010**, *35*, 959.
11. Matyjaszewski, K.; Xia, J. H. *Chem. Rev.* **2001**, *101*, 2921.
12. Wang, A. R.; Zhu, S. P. *Macromolecules* **2002**, *35*, 9926.
13. Wang, R.; Luo, Y. W.; Li, B. G.; Sun, X. Y.; Zhu, S. P. *Macromol. Theory Simul.* **2006**, *15*, 356.
14. Zhang, M.; Ray, W. H. *Ind. Eng. Chem. Res.* **2001**, *40*, 4336.
15. Zhou, Y. N.; Luo, Z. H. *Polym. Chem.* **2013**, *4*, 76.
16. Zhou, Y. N.; Luo, Z. H.; Chen J. H. *AIChE J.* **2013**, doi: 10.1002/aic.14057.
17. Zhu, S. P. *Macromol. Theory Simul.* **1999**, *8*, 29.
18. D'hooge, D. R.; Reyniers, M. F.; Marin, G. B. *Macromol. React. Eng.* **2009**, *3*, 185.
19. Delgadillo-Velazquez, O.; Vivaldo-Lima, E.; Quintero-Ortega, I. A.; Zhu, S. P. *AIChE J.* **2002**, *18*, 2597.
20. Zhang, M.; Ray, W. H. *J. Appl. Polym. Sci.* **2002**, *86*, 1630.
21. Wang, R.; Luo, Y. W.; Li, B. G.; Zhu, S. P. *AIChE J.* **2007**, *53*, 174.
22. Zhou, Y. N.; Li, J. J.; Luo, Z. H. *J. Polym. Sci. Part A: Polym. Chem.* **2012**, *50*, 3052.
23. Sun, X. Y.; Luo Y. W.; Wang, R.; Li, B. G.; Zhu, S. P. *Macromolecules* **2007**, *40*, 849.
24. Sun, X. Y.; Luo, Y. W.; Wang, R.; Li, B. G.; Zhu, S. P. *AIChE J.* **2008**, *54*, 1073.
25. D'hooge, D. R.; Reyniers, M. F.; Stadler, F. J.; Dervaux, B.; Bailly, C.; Prez, F. E. D.; Marin G. B. *Macromolecules* **2010**, *43*, 8766.
26. Zetterlund, P. B. *Macromolecules* **2010**, *43*, 1387.
27. Achilias, D. S.; Kiparissides, C. *J. Appl. Polym. Sci.* **1988**, *35*, 1303.
28. Duda, J. L.; Vrentas, J. S.; Ju, S. T.; Liu, H. T. *AIChE J.* **1982**, *28*, 279.
29. Hong, S. U. *Ind. Eng. Chem. Res.* **1995**, *34*, 2536.
30. Xue, C. M. Common Chemistry Handbook; Geological Press (Chinese): Beijing, **1997**; p 45.
31. Beuermann, S.; Buback, M.; Davis, T. P.; Gilbert, R. G.; Hutchinson, R. A.; Kajiwara, A.; Klumperman, B.; Russell, G. T. *Macromol. Chem. Phys.* **2000**, *201*, 1355.
32. Li, D. H.; Grady, M. C.; Hutchinson, R. A. *Ind. Eng. Chem. Res.* **2005**, *44*, 2506.
33. Buback, M.; Junkers, T. *Macromol. Chem. Phys.* **2006**, *207*, 1640.
34. He, T. Y. Master Dissertation, Xiamen University, Xiamen, China, **2008**.